Jurnal Teknologi

Full Paper

COMPARISON OF EXPERIMENTAL, 3D AND 1D MODEL FOR A MIXED-FLOW TURBINE UNDER PULSATING FLOW CONDITIONS

Meng Soon Chiong[a], Muhamad Hasbullah Padzillah[a*], Srithar Rajoo[a], Alessandro Romagnoli[b], Aaron W. Costall[c], Ricardo F. Martinez-Botas[c]

[a]UTM Centre for Low Carbon Transport in Cooperation with Imperial College London, Universiti Teknologi Malaysia, 81310 UTM Johor Bahru, Johor, Malaysia
[b]School of Mechanical and Aerospace Engineering, Nanyang Technological University, N3.2-02-32, 50 Nanyang Avenue, Singapore 639798, Singapore
[c]Department of Mechanical Engineering, Imperial College London, London SW7 2AZ, United Kingdom

Article history
Received
22 July 2015
Received in revised form
11 August 2015
Accepted
10 October 2015

*Corresponding author
mhasbullah@utm.my

Graphical abstract

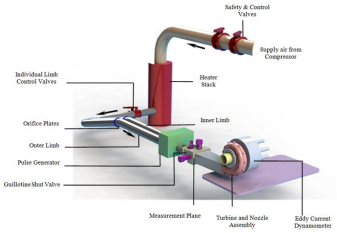

Abstract

The pulse flow performance of a turbocharger turbine is known to be different than its corresponding steady flow performance. This often leads to less-than-satisfactory 1D engine model prediction. In this study, the effectiveness of a 1D pulse flow turbine model is assessed against experimental data with the aid of 3D CFD model. The turbine under study is a single-entry variable geometry mixed-flow turbine. The result shows highly comparable pulse flow swallowing capacity and actual power characteristics between 1D and 3D models. The over-prediction in 1D actual power magnitude is found to be due to the simplification of combining nozzle and rotor stage pressure loss together.

Keywords: 1D, 3D, experiment, pulse flow, mixed-flow turbine

1.0 INTRODUCTION

Since the introduction of EURO 1 emissions legislation in 1993 till the recently implemented EURO 6, the pollutant emissions limit of automotive internal combustion engine (ICE), viz., particulate matter (PM) and NO_x levels have been cut down by nearly 95% [1]. While the upcoming legislation is still tentative at this stage, it is foreseen that the future focus will be shifted to increasing fuel economy and reducing CO_2 emissions. This comes as no surprise since CO_2 is the dominant greenhouse gas pollutant (82% as reported by [2]) among all four identified gases. The electricity and transportation sectors, being driven primarily by fossil fuels, are the largest CO_2 contributor.

Although electric vehicle is often regarded as the ultimate solution for zero-emissions transportation, this is not entirely true as long as the electricity sector is still relying on fossil fuel source [3]. For that reason, the conventional ICE is still likely to be the prime-mover in electrical and transportation sector for the next several decades to come [4].

Engine downsizing — reducing the engine displacement while maintaining the power and drivability of a larger engine — is seen to have the most optimum benefit-to-cost ratio among many other advance powertrain technologies [5]. Variable geometry turbine (VGT) technology is seen as an enabler for extreme engine downsizing in meeting the increasingly stringent emission regulations. Apart from its wider operating efficiency characteristics as a result of varying the turbine physical geometry, it has also

been regarded as a potential substitution for conventional turbocharger waste-gate in controlling the exhaust gas recirculation for emission management [6].

It has been shown that the use of variable geometry turbine over fixed geometry turbine (FGT) can yield lower engine smoke emission (typically suffered by diesel engine) at low speed operation and improve overall engine brake specific fuel consumption [7,8]. Moreover, 10% torque improvement throughout the engine operating speed is also experimentally shown to be possible, with additional achievable 5% suggested from numerical simulation [8]. In the application of exhaust waste heat energy recovery, particularly turbo-compounding, VGT is also found capable of improving the overall engine fuel consumption mainly owed to the varying swallowing capacity [9].

There are two variations of variable geometry turbine in general, viz., the sliding end-wall type or with pivoting nozzle vane type. Being more popular in small-to-medium size turbocharger turbine, the latter configuration will be studied in this paper. To date, the design of variable nozzle vane for passenger car application is still a challenging task, mainly because of its reliability issue under extreme operating condition, and the associated high production cost [6,10,11]. Nevertheless, the continuous effort from turbocharger manufacturers in developing a high-performance and high-reliability VGT is a good indication of its great potential in powertrain application for the years to come.

Due to the reciprocating motion of ICE, a turbocharger turbine is long known to operate at constantly pulsating flow condition. Its pulse flow performance, however, has been shown not to follow the steady flow characteristic [12,13]. Depending on the pulse flow frequency/unsteadiness, the instantaneous turbine performance is found to be influenced by the filling and emptying or wave action effect. Even though this does not raise additional concern in 3D computational fluid dynamic (CFD) since the entire turbine fluid domain has been accounted for, it does give quite significant impact on the calculation quality of a 1D engine gas dynamic code where the turbine sub-component is typically assumed to behave quasi-steadily.

One-dimensional engine cycle simulation is routinely employed in automotive industry for virtual engine design, initial performance and emissions studies, since it enables design-of-experiment type investigations to be carried out to establish the main component specifications (e.g., potential turbocharger options) and their trade-offs (e.g., surge margin vs. altitude capability), prior to expensive and time consuming test bed validation. Hence, the departure of turbine pulse flow performance from typical quasi-steady assumption may compromise the overall optimization of powertrain design. In regard of this deficiency, a validated 1D pulse flow turbine model has previously been developed for a single-entry nozzle-less turbine unit [14].

In this paper, the established 1D pulse flow turbine modeling methodology will be applied on a VGT. Its pulse flow performance will be verified against experimental data as well as 3D CFD model for detailed in-volute flow comparison. The objective is to identify any room of improvement for the 1D pulse flow model.

2.0 METHODOLOGY

The VGT used for the current study is an in-house designed single-entry volute and a variable nozzle vane assembly from Imperial College London [15]. The design was based on the nozzle-less unit tested by Szymko *et al.* [13]. Two different nozzle vane designs have been experimentally tested by Rajoo and Martinez-Botas [16], however the modeling work in this study will only emphasize on the more "efficient" design — the lean nozzle, which kept minimum vaneless inter-space. Although the subject VGT is a pivoting nozzle vane unit, the study will be conducted at constant nozzle vane angle. In the following subsections, the methodology of current study will be described. The experimental setup will first be discussed in Section 2.1. In Section 2.2, the details of 3D-CFD model will be presented, followed by the 1D modeling methodology in Section 2.3.

2.1 Experimental Setup

Figure 1 shows the schematics of the turbocharger test facility used in this research. The facility is located at Imperial College London for cold-flow testing and could be used for steady and pulsating flow testing. The compressed air for the test rig is supplied by three screw-type compressors with capacity up to 1 kg/s at maximum absolute pressure of 5 bars. The air is heated by a heater-stack to 330–345 K in order to prevent condensation during gas expansion in the turbine. The flow is then channeled into two 81.40mm limbs, namely outer and inner limb due to its relative position. This enables testing not only for single entry turbine but also for double or twin entry turbine.

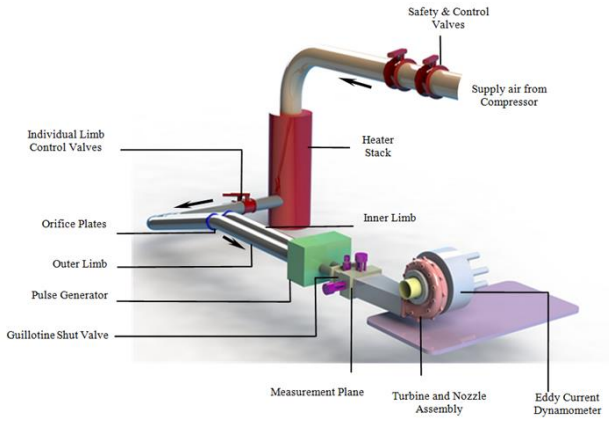

Figure 1 Imperial College 'cold flow' turbocharger test facility

The mass flow rate in both limbs is measured using both the v-cone flow meter and orifice plates. Downstream to the orifice plates is a pulse generator originally designed by Dale and Watson [12] in 1986. The pulse generator enables actual pressure pulse in the exhaust manifold to be replicated in the facility with the frequency up to 80Hz. For steady state testing, the pulse generator is defaulted to 'fully open' position to allow maximum steady-state flow area. Downstream of the pulse generator is the 'measurement plane', where all the parameters for the turbine inlet were acquired. This includes instantaneous total and static pressure sensors, thermocouples and also hotwire anemometer for instantaneous mass flow measurement.

The turbine is attached to a 60 kW eddy current dynamometer originally designed by Szymko *et al.* [17]. The whole assembly of dynamometer is placed on a gimbal bearing. The reaction force on the dynamometer assembly is measured by a 20 kg load cell where the rotor torque can be applied. The dynamometer also places a high flow rate water cooling system to disperse excessive heat absorbed by the magnetic plate. In addition, an optical sensor for instantaneous speed measurement is also installed within the dynamometer assembly.

2.2 Numerical Setup For 3D-CFD

The simulation works conducted in this research were executed using commercial 3D-CFD software — ANSYS CFX 14.1. The 3-D turbocharger turbine geometry consists of 5 main components which are the inlet duct, turbine volute, the aforementioned lean nozzle vanes and a mixed-flow turbine with 40mm chord length. The inlet duct and the volute were constructed using commercial computer-aided drafting software—SolidWorks and meshed using ANSYS ICEM CFD.

For the nozzle stage, 15 lean nozzle vanes were constructed by importing 3 profile lines into TurboGrid software where structured hexahedral meshed is automatically generated. Similar method is used to mesh the mixed flow turbine except 8 profile lines are needed due to its more complex geometry. The profile lines of the turbine blade were created using Bezier polynomial where its control points are shown in Figure 2.

Subsequently, all meshed components were assembled in ANSYS CFX-Pre as shown in Figure 3. The interfaces between each component are specified during this stage. The interfaces between inlet duct and volute, and also between volute to vane are specified as general connection. Transient interface is specified between vane and rotor domains with the specified time step of 10 of turbine rotation per time step.

At the domain inlet (inlet duct), instantaneous total pressure and total temperature are specified. The direction of inlet flow is defined so that the only velocity component that exists is normal to the inlet plane. The values for inlet boundary are taken directly from experimentally acquired values at the measurement plane. The outlet boundary condition requires the static pressure value. For this purpose, a constant atmospheric pressure is applied at the domain outlet. No-slip boundary condition is specified at all walls including vanes and rotor blades.

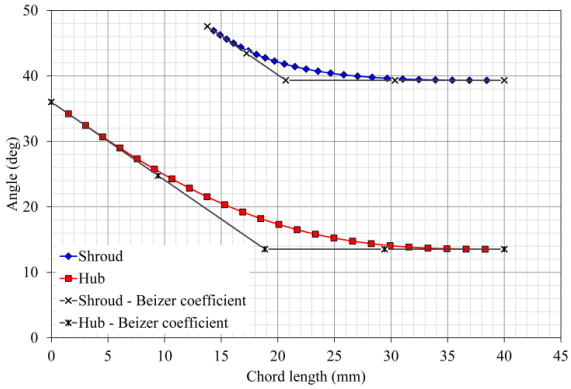

(a)

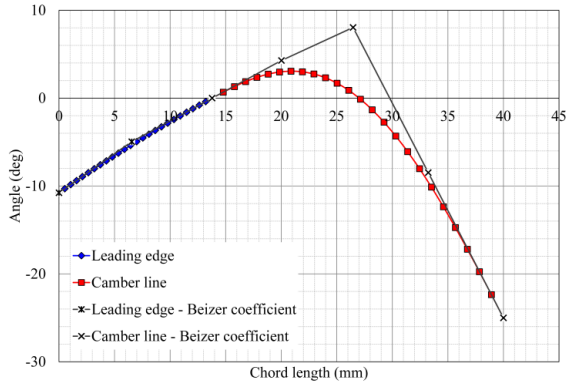

(b)

Figure 2 Development of turbine geometry using Bezier Polynomial

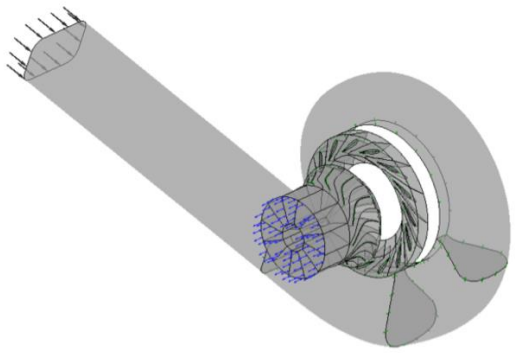

Figure 3 Assembly of domain in CFX-Pre

2.3 Numerical Setup For 1D Model

The computational tool used for 1D modeling is the Imperial College London proprietary one-dimensional wave action simulator [18]. The simulator is based on the one-dimensional Euler formulation and features second order accurate numerical scheme coupled

with total variation diminishing (TVD) flux limiter, thus ensuring conservative and shock-capturing solutions.

The 1D model domain will follow the latest computation domain established in [14], as illustrated in Figure 4. The volute domain is modelled as series of pipes with varying areas in accordance to actual unit reported in [15]. The flow from the turbine inlet is assumed to merge into a single pipe from four rotor entries located at 90°, 180°, 270° and 360° azimuth angle before entering the nozzle and rotor boundary.

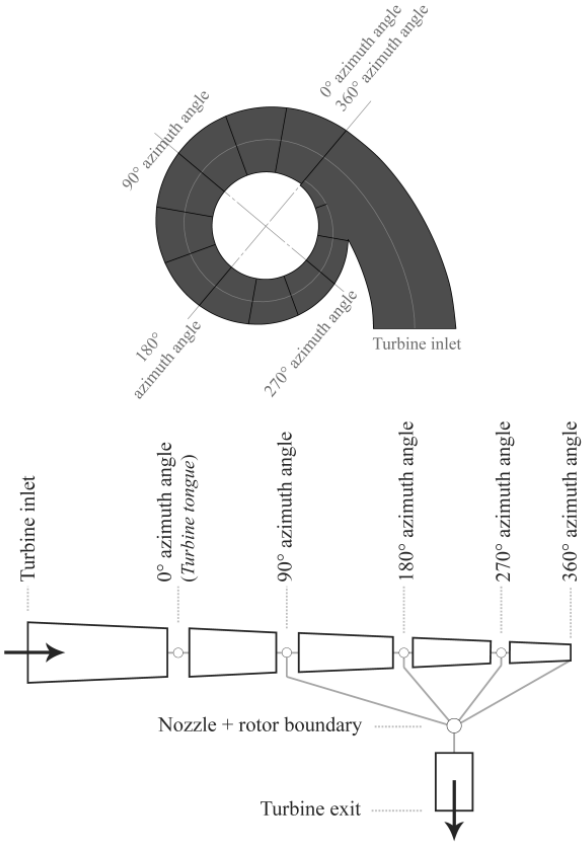

Figure 4 1D model computation domain

The exit flow at nozzle trailing edge is found not follow the exact nozzle angle and the deviation changes with different mass flow operating condition [19]. However, it is tedious to vary the 1D model cross-sectional area (trailing edge) of the nozzle model in real time, which requires precise evaluation of resultant effective flow area. In view of this difficulty, it seems more sensible to assume the nozzle and rotor stages to behave quasi-steadily, without compromising the model performance quality. Furthermore, Strouhal no. analyses found in literature [13, 20] suggest that the unsteadiness effect is only noteworthy if the gas flow path length is significantly large compared to the flow disturbance, e.g., across the volute stage. Since the nozzle mean chord length is only ~30% of the rotor passage length, the flow characteristic across the nozzle stage is almost certain to behave quasi-steadily.

The combined pressure loss coefficient and specific power parameter (defined in Equations 1 and 2) across nozzle and rotor stage for the turbine which operate at 60° nozzle angle of 26.9 rps/√K turbine speed is given in Figure 5. Subscript 1 and 2 denote the nozzle and rotor stage upstream and downstream respectively. Note that the pressure loss coefficient here accounts for the nozzle and rotor stage. The specific power parameter however, is only contributed by the rotor stage since no work transfer is associated with nozzle stage. The steady flow validation of 1D model will be presented in Section 3.1 comparing against 3D-CFD model prediction and experimental data.

$$\text{Pressure loss coefficient} = \frac{\kappa(p_1 - p_2)}{\rho_1 u_1^2} \quad (1)$$

$$\text{Specific power parameter} = \frac{h_{01} - h_{02}}{T_{01}} \quad (2)$$

where h_0 = stagnation enthalpy
p = static pressure
T_0 = stagnation temperature
u = flow velocity
ρ = flow density

3.0 RESULTS AND DISCUSSION

In this section, the steady and pulse flow performance comparison between experimental data, 1D and 3D model performance will be compared and discussed.

3.1 Steady Flow Validation

The validation of steady flow performance between 1D and 3D model to experimental data at 60° nozzle angle of 26.9 rps/√K turbine speed is shown in Figure 6. In general, both models matched the experimental steady flow swallowing capacity very well with maximum deviation of 0.22 kg√K/s-bar seen at pressure ratio, PR = 1.58 in Figure 6a from 3D-CFD model. The turbine total-static efficiency validation, as shown in Figure 6b, also indicates that both 1D and 3D models matched the subject turbine performance reasonably. The maximum efficiency deviation from experimental data for both models were recorded at the lowest PR points (+11.5% for 1D model and -8.8% for 3D model). However, it is worth mentioning that the typical uncertainty of the test facility at such PR range and 26.9 rps/√K operating speed is approximately ±7% [13].

Additionally, the comparison of static pressure at 180° volute azimuth angle between 1D and 3D model is given in Figure 7. This comparison gives a good indication on how well the heavily simplified 1D domain in simulating the primary flow changes of the complex 3D turbine volute. From Figure 7, it can be seen that the 1D model successfully captured the local static pressure variation throughout the entire PR operating range across the volute stage. Such observations further strengthened the validity of 1D model domain in Figure 4 for a single-entry turbine.

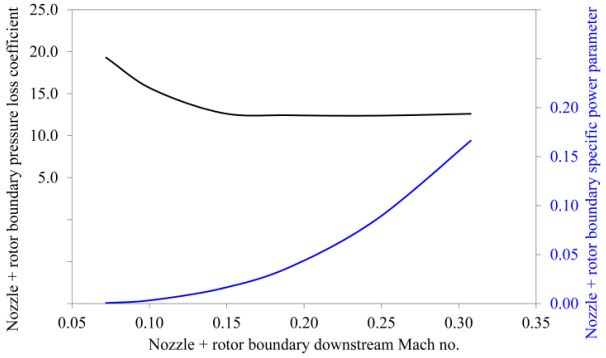

Figure 5 The nozzle + rotor boundary pressure loss coefficient and specific power parameter at 60° nozzle angle of 26.9 rps/√K turbine speed

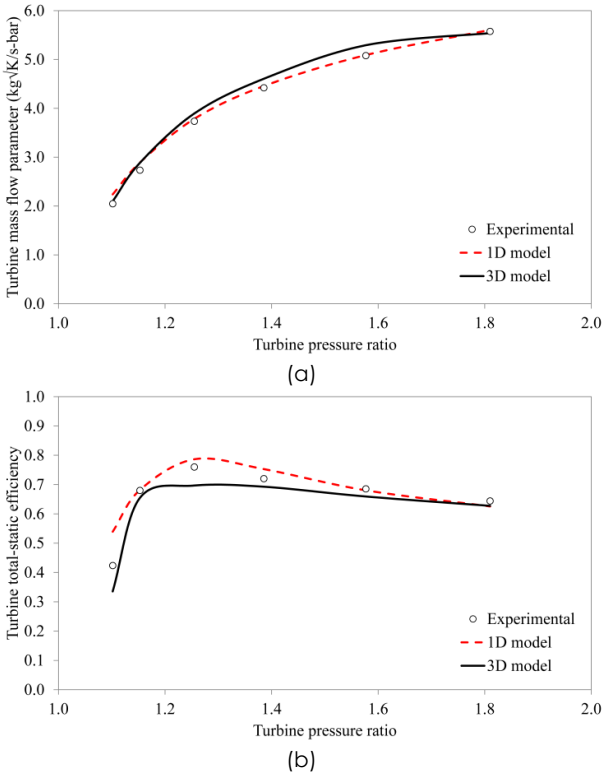

Figure 6 Steady flow validation of 1D and 3D model against experimental data (a) turbine mass flow parameter and (b) turbine efficiency

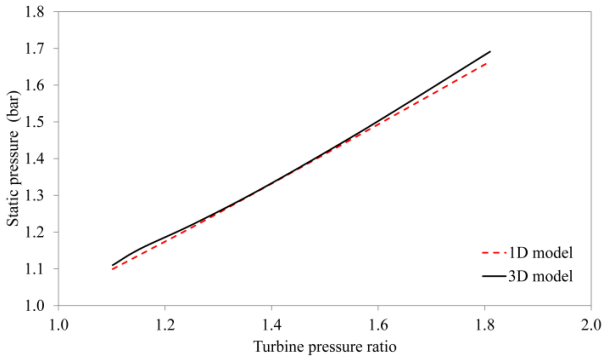

Figure 7 Comparison of volute static pressure at 180° azimuth angle between 1D and 3D model

3.2 Pulse Flow Performance Comparison

The pulse flow performance of 1D and 3D model is evaluated against experimental data at 20 Hz pulse frequency. As mentioned earlier in Section 2.2, the instantaneous experimental stagnation flow condition (shown in Figure 8) at test facility measurement plane (illustrated in Figure 1) were used as the inlet boundary conditions of both 1D and 3D model to achieve the same comparison basis against experimental data. In doing so, the resultant instantaneous inlet mass flow rate comparison will indicate the effectiveness of model domain in rendering the turbine swallowing capacity. This would consequently influence the quality of instantaneous actual power prediction at rotor wheel further downstream.

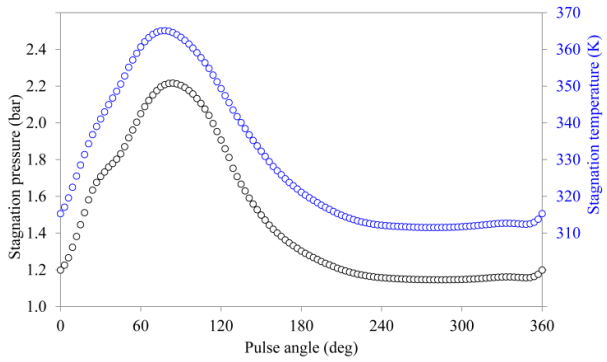

Figure 8 Model inlet boundary stagnation pressure and temperature

The instantaneous mass flow rate at turbine inlet for 1D and 3D model predictions and experimental data are shown in Figure 9a. The mass flow rate profile is shown for one single pulse where the pulse angle is normalized to 360° for a complete cycle. At first glance, it can be seen that the prediction from 1D and 3D models are in good agreement with one other in term of mass flow amplitude and the phasing of filling and emptying process. In comparison to experimental data, the pulse mass flow characteristic is also considerably well captured by both models. Of great interest here is the small trough at pulse pressure peak during 40°–60° pulse angle. While there is no such secondary fluctuation visible in the model inlet boundary condition (in Figure 8), this secondary trough must be due to the wave action in turbine volute as the pulse flow propagates along it. The observation of earlier emptying prediction than experimental data was also previously reported for a nozzle-less turbine modeling at the same pulse frequency but at higher operating speeds [14].

The comparison of instantaneous actual power between 1D and 3D model predictions and experimental data are shown in Figure 9b. Note that the actual power profiles are shown in their actual phasing, i.e., without applying any phase-shifting, hence appeared to be lagged behind the mass flow rate profile in Figure 9a. It can be seen that the pulse feature and phasing of 1D and 3D model predictions

are highly comparable, despite that the 1D prediction shows much higher peak magnitude (by about +15.5%). It is obvious that the small trough at pulse peak seen in inlet mass flow rate has been damped out significantly as the pulse flow travels downstream into the rotor wheel.

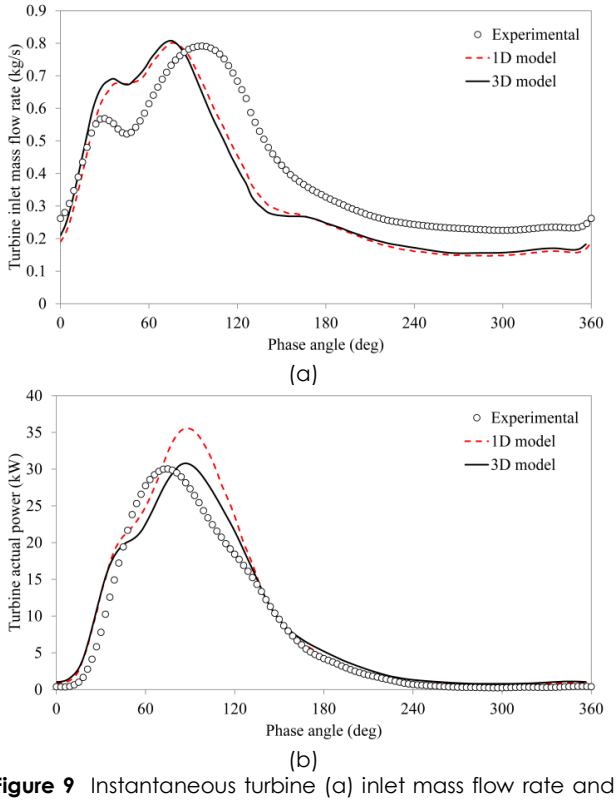

Figure 9 Instantaneous turbine (a) inlet mass flow rate and (b) actual power comparison between 1D and 3D prediction and experimental data

On the other hand, the 3D model prediction shows closer peak magnitude compared to experimental data, with mere over-prediction of +2.47%. However, there are approximately 15° of phase difference in between experimental and 3D model prediction pulse peak. It is also noted that the small trough in experimental inlet mass flow has been completely damped out.

The departure of turbine pulse flow performance from corresponding steady flow performance can be more clearly shown in the hysteresis plot. This is shown in Figures 10a and 10b for the turbine mass flow parameter and actual power respectively. In line with the literature findings [13], the swallowing capacity hysteresis curve from 1D and 3D model predictions are of the same characteristic at 20 Hz pulse frequency and 26.9 rps/√K operating speed. Particularly, the hysteresis curve is encapsulating the steady-state performance line — typical filling and emptying phenomenon.

On the other hand, the experimental swallowing capacity hysteresis shows there is a cross over between the filling and emptying line at PR = 1.64. In addition, the entire hysteresis loop is found to be much higher than the steady flow performance line. Despite so, the actual power hysteresis curves (shown in Figure 10b) for experimental data, 1D and 3D models are relatively closer to one another. One important observation here is that the instantaneous actual power only start to develop at PR = ~1.6, which leads to opposite hysteresis direction than the swallowing capacity in Figure 10a. This is due to the phase difference between the turbine inlet mass flow rate and the actual power extracted at rotor wheel. It is also important to point out that all the hysteresis loops in Figure 10b are encapsulating the steady flow performance line as a result of the filling and emptying effect.

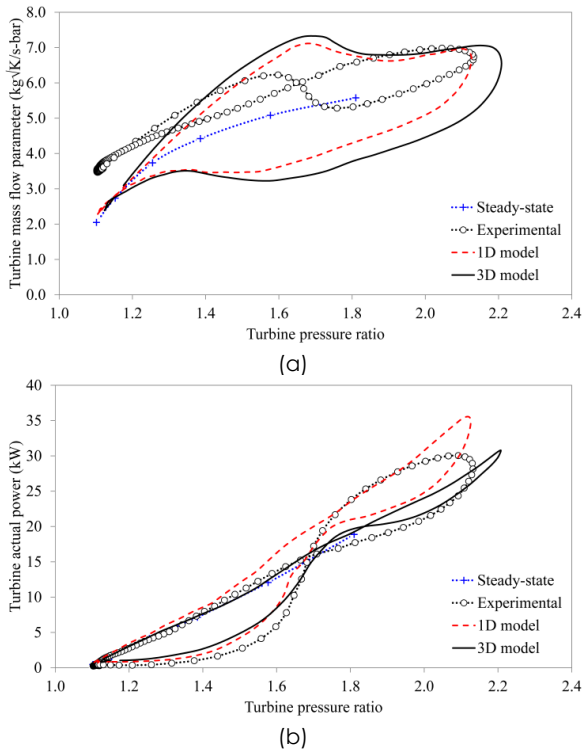

Figure 10 Turbine pulse flow (a) swallowing capacity and (b) actual power hysteresis comparison between 1D and 3D prediction, experimental data and steady flow performance data

To further identify the cause of over-prediction in actual power peak by 1D model seen in Figures 9b and 10b, the in-volute pulse pressure is compared against 3D model data in Figure 11. Looking at the pulse pressure at 180° volute azimuth angle, it is clear that the 1D model domain is satisfactory resembling the pulse pressure changes. This is reflected as the reasonable peak pressure magnitude and the formation of small trough before 60° pulse angle at the pulse rising edge.

The pulse pressure at nozzle leading edge and at the nozzle-to-rotor interspace is also shown for 3D model in Figure 11. Since the nozzle and rotor stage in 1D model is assumed to be one single quasi-steady boundary, the pulse pressure at nozzle-to-rotor interspace cannot be extracted. From Figure 11, it can be seen that the

static pressure change as the flow approaching the nozzle leading edge from volute centroid is rather significant. Thus, it is apparent from this comparison that the pressure loss for nozzle and rotor stage must be treated separately. As a result, the flow state across the rotor stage can be anticipated to be lower than the current prediction.

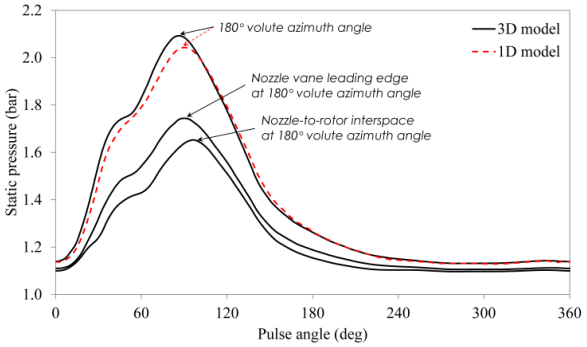

Figure 11 In-volute pulse pressure comparison between 1D and 3D model

4.0 CONCLUSION

In this paper, the pulse flow performance for a VGT at 20 Hz pulse flow of 26.9 rps/√K operating speed from experimental testing and 1D and 3D numerical modeling are presented. The 1D and 3D numerical model performances are first validated at steady flow operating condition and then used for pulse flow prediction. From the result comparisons, the following conclusions can be drawn:

1. The instantaneous turbine inlet mass flow rate predictions from 1D and 3D models are highly comparable. This indicates the 1D model domain is sufficiently representative despite it has been heavily simplified down to one-dimensional.
2. The instantaneous turbine actual power predictions from 1D and 3D models are in the correct phasing with experimental data. This shows the capability of:
   i. 1D model domain in capturing the correct phasing of energy transfer into rotor wheel and
   ii. The effectiveness of 3D model in predicting instantaneous turbine flow state under pulse flow operating condition.
3. The over-prediction of actual power magnitude by 1D model is identified to be due to the simplification of assuming the nozzle and rotor stage to be one single quasi-steady boundary.
4. For future improvement on the 1D pulse flow model performance, it is suggested that the nozzle stage pressure loss has to be treated separately, despite the flow state across it is still behaving quasi-steadily.

Acknowledgement

The authors would like to thank Universiti Teknologi Malaysia for Flagship Grant VOT 4L174.

References

[1] Hogg, R. 2014. *Life Beyond Euro VI*. URL http://www.automotiveworld.com/megatrends-articles/life-beyond-euro-vi/ last accessed 13.07.15.
[2] US Environmental Protection Agency. 2015. *Carbon Pollution Standards*. URL http:// www2. epa. gov/ sites/ production/ files/ 2014-05/ ghg-chart.png last accessed 13.07.15.
[3] Jaffe, E. 2015. *Where Electric Vehicles Actually Cause More Pollution than GasCcars*. URL http:// www. citylab. com/ weather/ 2015/ 06/ where- electric- vehicles- actually-cause- more- pollution- than-gas-cars/397136/ last accessed 13.07.15.
[4] Markus, F. 2015. *Mousetrap Betterment: Keeping Combustion Contemporary — Technologue*. URL http:// blogs. motortrend. com/ 1506_ mousetrap_ betterment_ keeping_ combustion_ contemporary_ technologue. html last accessed 13.07.15.
[5] KPMG International 2010. *The Transformation of the Automotive Industry: The Environmental Regulation Effect. Executive Summary*.
[6] Jinnai, Y., Arimizu, H., Tashiro, N., Tojo, M., Yokoyama, T. and Hayashi, N. 2012. A Variable Geometry (GV) Turbocharger for Passenger Cars to Meet European Union Emission Regulations. *Mitsubishi Heavy Industries Technical Review*. 49(2): 17–26.
[7] Matsumoto, K., Jinnai, Y. and Suzuki, H. 1998. Development of Variable Geometry Turbocharger for Diesel Passenger Car. *Proceedings of IMechE 6th International Conference on Turbocharging and Air Management Systems*. Paper C554/005.
[8] Hawley, J. G., Cox, A., Pease, A. C., Bird, G. L. and Horrocks, R. W. 1998. Use of a VGT to Improve the Limiting Torque Characteristics of a D1 Automotive Diesel Engine. *Proceedings of IMechE 6th International Conference on Turbocharging and Air Management Systems*. Paper C554/014.
[9] Zhao, R., Zhuge, W., Zhang, Y., Yang, M., Martinez-Botas, R. F. and Yin, Y. 2015. Study of Two-Stage Turbine Characteristic and Its Influence on Turbo-Compound Engine Performance. *Energy Conversion and Management*. 95: 414-423.
[10] Osako, K., Samata, A., Ibaraki, S., Jinnai, Y., Suzuki, H. and Hayashi, N. 2006. Development of the High-Performance and High-Reliability VG Turbocharger for Automotive Applications. *Mitsubishi Heavy Industries Technical Review*. 43(3): 1–5.
[11] Tomohiro, I., Yuuji, K., Yoshimitsu, M. and Yasutaka, S. 2011. Development of VGS unit (STEP4) for RHV4 Turbocharger. *IHI Engineering Review*. 44(2): 1–6.
[12] Dale, A. and Watson, N. 1986. Vaneless Radial Turbocharger Turbine Performance. *Proceedings of the IMechE 3rd International Conference on Turbocharging and Turbochargers*. Paper C110/86.
[13] Szymko, S., Martinez-Botas, R. F. and Pullen, K. R. 2005. Experimental Evaluation of Turbocharger Turbine Performance under Pulsating Flow Conditions. *Proceedings of the ASME Turbo Expo 2005: Power for Land, Sea and Air*. Paper GT2005-68878.
[14] Chiong, M. S., Rajoo, S., Romagnoli, A., Costall, A. W., and Martinez-Botas, R. F. 2015. Non-Adiabatic Pressure Loss Boundary Condition for Modeling Turbocharger Turbine Pulsating Flow. *Energy Conversion and Management*. 93:267–281.
[15] Rajoo, S. 2007. *Steady and Pulsating Performance of a Variable Geometry Mixed Flow Turbocharger Turbine*. Ph.D. Thesis. Imperial College, University of London.

[16] Rajoo, S. and Martinez-Botas, R. F. 2008. Variable Geometry Mixed Flow Turbine for Turbochargers: An Experimental Study. *International Journal of Fluid Machinery and Systems*. 1: 155-168.
[17] Szymko, S., McGlashan, N. R., Martinez-Botas, R. F. and Pullen, K. R. 2007. The Development of Dynamometer for Torque Measurement of Automotive Turbocharger Turbines. *Proceedings of the Institution of Mechanical Engineers, Part D: Journal of Automobile Engineering*. 221(2): 225–239.
[18] Costall, A. W. 2007. *A One-Dimensional Study of Unsteady Wave Propagation in Turbocharger Turbines*. Ph.D. Thesis. Imperial College, University of London.
[19] Hideaki, T., Masaru, U., Akira, I. and Shinnosuke, I. 2007. Study on Flow Field in Variable Area Nozzle for Radial Turbines. *IHI Engineering Review*. 40(2): 89–97.
[20] Chen, H. 1990. *Steady and Unsteady Performance of Vaneless Casing Radial-Inflow Turbines*. Ph.D. Thesis. UMIST, University of Manchester.